Transmissible Ileal Hyperplasia of Hamsters

II. Ultrastructure

Elizabeth A. Johnson, MS, and Robert O. Jacoby, DVM, PhD

The ultrastructure of developing ileal lesions was characterized in weanling hamsters with experimentally induced transmissible ileal hyperplasia (TIH). The primary lesion was mucosal hyperplasia with progressive replacement of mature villus columnar absorptive cells by undifferentiated crypt-type cells. The undifferentiated, mitotically active cells expanded onto villus walls from their normal location in crypts by Day 10 and reached villus tips by Day 14. Aggregates of slightly curved, 0.3 × 1.5 μ, rod-shaped bacteria were detected in the apical cytoplasm of crypt epithelium by Day 5. They replicated intracellularly and accumulated in progressively greater numbers in hyperplastic cells. Active penetration of cells by intralumenal bacteria was not seen. The appearance and distribution of TIH-associated antigen, demonstrated by indirect immunofluorescence, was identical to that observed for intracellular bacteria. Hyperplastic, bacteria-laden crypt epithelium penetrated adjacent supporting tissues. Dilated crypts with flattened epithelium ruptured and released organisms into surrounding tissues. Pyogranulomatous inflammation began at 17 to 25 days and preceded or accompanied penetration of the muscle layers by expanding crypts. Macrophages and neutrophils in inflammatory lesions contained many phagocytized bacteria. In some advanced lesions mature, bacteria-free absorptive cells and goblet cells reappeared. These observations support the hypothesis that intestinal bacteria cause TIH. (Am J Pathol 91:451–468, 1978)

TRANSMISSIBLE ILEAL HYPERPLASIA (TIH) is a common, naturally occurring disease of weanling hamsters.[1-3] The preceding paper[4] confirmed that the primary lesion in TIH is severe hyperplasia of ileal mucosa, with penetration of connective tissue and muscular layers by fronds of hyperplastic epithelium. Mucosal proliferation is followed by pyogranulomatous inflammation. Hyperplasia is associated with accumulation of particulate antigen (TIH-associated antigen) in the cytoplasm of ileal mucosal epthelial cells. Histologic studies indicated that the accumulations and localization of antigen in hyperplastic epithelium correlated closely with the appearance of intracytoplasmic bodies resembling bacteria.[4] This report is the first description of the ultrastructural morphogenesis of TIH. It shows that bacteria invade ileal epithelium before hyperplasia begins and confirms that in mucosal epithelium, the develop-

From the Section of Comparative Medicine, Yale University School of Medicine, 375 Congress Avenue, New Haven, Connecticut.

Presented in part at the 28th Annual Session of the American Association for Laboratory Animal Science, Anaheim, Calif., October 1977.

Supported by Grants RR00945, RR00393, and RR05358 from the Public Health Service.

Address reprint requests to Dr. Robert O. Jacoby, Section of Comparative Medicine, Yale University School of Medicine, 375 Congress Ave., New Haven, CT 06510.

0002-9440/78/0608-0451$01.00

ment and distribution of TIH-associated antigen coincides with that of intracellular bacteria. The findings support the hypothesis that bacteria cause TIH.

Materials and Methods

Animals

Male weanling Lak:LVG(Syr) hamsters weighing 25 to 30 g (Lakeview Hamster Colony, Newfield, N.J.) were housed as previously described [4] and fed a semisynthetic hamster diet formulated by Dr. Paul Newberne at the Massachusetts Institute of Technology. Preliminary trials with the diet indicated that the diet neither altered the morphology of TIH nor induced TIH in hamsters inoculated with homogenates of normal ileum.

Animal Inoculation

Ileal homogenate was prepared as previously described.[4] Forty-eight hamsters were gavaged with 1.0 ml of homogenate. Thirteen control hamsters were gavaged with 1.0 ml of homogenized normal ileum.

Transmission Electron Microscopy

Hamsters were randomly selected for necropsy at 4- to 5-day intervals and were killed with ether. The terminal ileum with ileocecal junction, mesenteric lymph node, and liver were removed immediately. The ileum was split longitudinally. One half was placed in 2% osmium in 0.1 M phosphate buffer, pH 7.25, and one half was immersed in iced 4% formaldehyde and 1% glutaraldehyde prepared with 200 mOsm phosphate buffer, pH 7.2.[5] After 5 to 15 minutes of fixation, 1-mm transverse sections of ileum and longitudinal sections of ileocecal junction were fixed for 60 minutes in osmium or for 3 hours in formaldehyde–glutaraldehyde. Mesenteric lymph node and liver were minced and fixed in formalin–glutaraldehyde for 4 hours. Aldehyde-fixed tissues were washed twice in 0.1 M Millonig's buffer, pH 7.25, and postfixed in 2% osmium in the same buffer for 45 minutes. After two more washes in Millonig's buffer, tissues were dehydrated through graded alcohols and propylene oxide and embedded in Epon–Araldite.[6] Sections 2-μ thick were stained with 1% methylene blue [7] or with toluidine blue. Specimens in which epithelium could be followed from crypt bases to adjacent villus tips were trimmed, thin-sectioned on an LKB Ultrotome III (LKB Instruments, Rockville, Md.), and picked up on naked 150-mesh grids. They were stained with alcoholic uranyl acetate and lead citrate [8] and examined in either a Hitachi HU11, HU8 (Hitachi, Ltd., Tokyo, Japan) or Philips 201 electron microscope (N.U. Philips, Co., Eindhoven, the Netherlands).

Scanning Electron Microscopy

Portions of terminal ileum were opened longitudinally and pinned to paraffin blocks. The mucosal surface was flushed with formaldehyde–glutaraldehyde, and the block was immersed in fixative for 4 hours. It was washed twice in 0.1 M Millonig's buffer and postfixed in 2% osmium in 0.1 M Millonig's buffer. Samples were rinsed 10 times in buffer and incubated for 10 minutes with distilled water, immersed in 1% OsO_4 for 1 hour, rinsed twice in buffer, and dehydrated in graded alcohols. Samples were dried by the critical point method, mounted on stubs, coated with gold–palladium, and viewed with an Autoscan scanning electron microscope (ETEC Corp., Hayward, Calif.).

Light and Fluorescence Microscopy

Segments of terminal ileum were examined by light or fluorescence microscopy as previously described.[4] Selected sections were stained with periodic acid–Schiff (PAS) stain.

Results

Ultrastructure of Ileal Mucosal Epithelium From Control Hamsters

Crypts were lined by a single layer of undifferentiated pyramidal or columnar cells resting on a thin basement membrane (Figure 1). The lumenal segment of plasma membrane was composed of short irregularly spaced microvilli. Lateral plasma membranes were straight, with some basal interdigitations, and cells were joined by desmosomes and terminal bars. The nucleus of a typical crypt cell was oval and basilar with emarginated chromatin and one or two prominent nucleoli. The cytoplasm contained numerous free ribosomes, a perinuclear Golgi apparatus, and moderate numbers of mitochondria. Paneth cells with large secretory granules and extensive rough endoplasmic reticulum (RER) were seen at the base of many crypts (Figure 1). The midcrypt region contained many dividing cells. The transition to more differentiated cells was gradual and occurred primarily in the upper crypt compartment. Microvilli became taller and more numerous, and mature absorptive cells covering villi had a uniform brush border (Figure 2). Villus cells were more cuboidal than crypt cells and their nuclei were more centrally located. Lateral plasma membranes between adjacent cells were convoluted and interdigitated. In the cytoplasm, a terminal web developed beneath the microvillus border and mitochondria and short segments of RER were prominent. Cells in mitosis were not seen. Goblet cells and enteroendocrine cells were seen occasionally in crypts and along lower segments of villi (Figure 2). Degenerating cells were sometimes seen in the extrusion zone at the villus tip.

Association of Intracellular Bacteria With Development of Mucosal Hyperplasia

Bacteria were seen in the apical cytoplasm of mucosal epithelial cells of infected hamsters by 5 days after inoculation. They were straight or slightly curved cylindric rods with crenulated cell walls and rounded, slightly tapered ends (Figure 3). They measured 0.3 to 0.4 $\times$ 1.4 to 2.3 μ and divided intracellularly by binary fission (Figure 4). An electron-lucent halo surrounded each organism in some aldehyde-fixed tissues, but it was not seen in specimens fixed in osmium alone. Bacteria were not segregated by intracytoplasmic membranes unless secondary lysosomes developed. Bacteria were not detected invading cells or passing between cells; however, morphologically identical organisms were seen in the crypt lumen.

Intracellular bacteria were located primarily in crypt epithelium at Day 5 (Figure 5). Few crypts were infected, and bacteria were typically observed in groups of several adjacent cells, including cells in mitosis. Some crypt–villus units were more extensively infected, and cells containing organisms extended from crypt base to villus tip. In the extensively infected units, bacteria were more numerous in mature absorptive cells (Figure 6) than in undifferentiated crypt cells. Intracellular bacteria were not observed in ileal epithelium from control hamsters. Intracellular agents such as viruses or protozoa were not detected in either hyperplastic or normal ileal mucosal epithelium.

Development of Hyperplasia

Hyperplasia began by Day 10 with proliferation of undifferentiated crypt cells and elongation of crypts. There was a multifocal distribution of affected crypt–villus units. All hyperplastic units contained intracytoplasmic bacteria, and hyperplasia was never observed in crypt–villus units without bacteria. Occasionally, groups of uninfected cells were seen along infected segments of crypt or villus epithelium. Uninfected cells were always better differentiated than adjacent infected cells, particularly along the brush border (Figure 7).

Between 10 and 14 days after inculation, normal villus epithelium was gradually replaced by hyperplastic epithelium containing intracellular bacteria. Hyperplastic cells were elongated and appeared pseudostratified, particularly in cryptal regions (Figure 8). Most cells, however, abutted the basement membrane except cells in mitosis, which were periluminal and often separated from the basement membrane by an underlying cell. Hyperplastic cells resembled undifferentiated crypt epithelium with an abundance of free ribosomes and irregular microvillar borders (Figure 9). They extended to villus tips in some animals, while in others the tips of villi were covered by extremely dense, partially differentiated epithelium with increased numbers of stubby microvilli. In all cells, bacteria were most numerous in the apical cytoplasm but were occasionally seen in secondary lysosomes near the nucleus. Necrotic cells were also common in the lower half of the crypt–villus units. Some were shed into the intestinal lumen, whereas others were phagocytized by adjacent cells (Figure 8).

Hyperplasia developed in the duodenum and jejunum of 2 infected hamsters. Elongated villi were covered by undifferentiated cells containing numerous bacteria in the apical cytoplasm. Bacteria were morphologically identical to those seen in lesions of the terminal ileum.

Penetration of Supporting Tissues by Hyperplastic Epithelium and Development of Inflammation

Hyperplastic, bacteria-laden crypts began to penetrate muscularis mucosa by Day 17. The penetrating epithelium was frequently flattened and the supporting basement membrane was thin and focally dissoluted (Figure 10). There was focal necrosis of crypt epithelial cells and extracellular bacteria were seen between myofibers. Macrophages and neutrophils which infiltrated ruptured crypts, villus lamina propria, submucosa, and adjacent muscle tunics contained large phagosomes filled with partially degraded bacteria (Figure 13). Their cytoplasm contained numerous PAS-positive granules.

In several fully developed lesions (Day 25) goblet cells or mature columnar absorptive cells appeared along segments of bacteria-laden hyperplastic epithelium (Figure 11). They were seen primarily in crypt and lower villus regions. They were free of cytoplasmic bacteria but frequently contained lysosomes with bacterial remnants. The brush border and associated glycocalyx were well developed in these cells compared with adjacent infected cells (Figure 12).

Scanning Electron Microscopy

In control hamsters, short, closely spaced villi projected into the intestinal lumen (Figure 14) and in some areas narrow crypt orifices could be seen at the bases of villi. Villi tapered toward the tips and were slightly flattened. A deep fold encompassed the base of most villi and there were shallower transverse infoldings on villus surfaces. A layer of tightly packed microvilli covered all villi and intervillus spaces (Figure 15). Early hyperplastic changes in crypt and lower villus detected by transmission electron microscopy were not apparent. However, pronounced alterations in villus structure occurred in more advanced lesions. Villi became elongated, broader, and flatter, and the crypt–villus junction was elevated above the basal lamina (Figure 17).

Blocks of tissue were fractured after critical-point drying to expose longitudinal sections of crypt–villus units. Some crypts were four to five times normal length and only rudimentary villi remained at the surface. Other areas were comprised of leaf-like villi or plateaus formed by villus fusion and punctuated by small irregular crevices (Figure 16). Hemorrhage, cellular debris, and bacteria obscured the surface of many advanced lesions.

At higher magnification, cells covering normal villi had a well-developed, uniform microvillus border, whereas microvilli on villi covered by hyperplastic cells were sparse (Figure 18). The diameter of hyperplastic

cells was decreased compared with normal absorptive cells, and their lateral cell membranes were more prominent.

Immunofluorescence

The appearance and distribution of TIH-associated fluorescent antigen was identical to that described in the preceding paper except that antigen was detected in 2 of 4 animals examined as early as Day 5.

Discussion

Several findings from the present study offer support for the hypothesis that bacteria cause TIH. First, bacteria were detected in crypt cells by 5 days after inoculation, but hyperplasia was not found until Day 10. Second, all hyperplastic cells contained intracytoplasmic bacteria, whereas hyperplasia was never observed in uninfected crypt–villus units from TIH-infected hamsters or in ileal mucosa from control hamsters. Third, hyperplastic lesions developed in the duodenum and jejunum of 2 hamsters and both contained large numbers of intracytoplasmic bacteria morphologically identical to those in ileal lesions. Fourth, infected hyperplastic villus epithelial cells were either undifferentiated or poorly differentiated, whereas complete differentiation was seen only among groups of uninfected cells in advanced lesions. Finally, no other intracellular infectious agents such as viruses or protozoa were detected in either hyperplastic or normal ileal mucosa.

Previous studies have also suggested that bacteria contribute to the etiology of TIH. Wagner and co-workers detected intracellular bacteria in ileal mucosal epithelium of hamsters with naturally occurring TIH,[9] but correlations between the distribution of organisms and lesions and between invasion of organisms and development of hyperplasia were not explored. Jacoby and others found gram-negative intracytoplasmic bacteria in lesions from hamsters with experimentally induced TIH [4] and also reported that TIH was induced by repeatedly freeze-thawed supernatants of homogenized ileal lesions but that infectivity was abrogated by heating supernatants at 56 C for 30 minutes or by passing them through bacteria-retaining filters.[3] The intracellular bacteria associated with TIH are compatible morphologically with gram-negative rods,[10] but they have not yet been identified. Intracellular bacteria have also been detected by electron microscopy in the ileal mucosa of pigs with intestinal adenomatosis, a proliferative lesion closely resembling TIH.[11,12] *Campylobacter sputorum mucosalis* was isolated from ileal lesions,[13] but there are no reports of experimental transmission of the disease by this organism.

We had previously shown that there is a close association between the

development and distribution of particulate TIH-associated antigen and the development of hyperplasia.[3,4] Results reported here confirm that the distribution of TIH-associated antigen corresponds identically to the distribution of intracytoplasmic bacteria in mucosal epithelium. They showed that PAS-positive macrophages in granulomatous lesions which contained TIH-associated antigen [4] were filled with large secondary lysosomes containing partially digested bacteria. Therefore, TIH-associated antigen is likely the intracellular bacterium.

It is not clear how bacteria infect epithelial cells in TIH. Bacteria were not seen invading cells or in close association with the brush border as reported for enteric pathogens such as *Salmonella typhimurium, Shigella flexneri,* or *Escherichia coli.*[14-16] TIH-associated bacteria were not enclosed in host cell membranes unless secondary lysosomes developed, whereas intracellular enteric bacteria are commonly in phagocytic vacuoles. In addition, bacteria were always observed in ribbons of infected cells and had a predilection for crypt cells. This observation speaks against a random distribution of penetration by intralumenal organisms. A more likely possibility is that bacteria enter a few crypt cells, eg, by phagocytosis, soon after hamsters are inoculated, so the chance of observing penetration is small. Intracellular replication of organisms may rupture the phagocytic vacuole, leaving them in intimate contact with the cytoplasm. If bacterial replication proceeds in undifferentiated dividing crypt cells, a pool of infected cells would be available to migrate onto villus walls.

Many enteric bacteria which penetrate mucosal epithelium produce cytolytic changes.[14-17] In contrast, TIH-associated bacteria are associated primarily with hyperplastic changes. Cell necrosis is variable and usually follows development of hyperplasia. Nevertheless, large secondary lysosomes containing bacteria and cell debris form in epithelial cells. They probably correspond to the so-called intracytoplasmic bodies or inclusions observed in histologic sections.[3,4]

TIH is characterized by mucosal hyperplasia which begins in the crypt cell compartment. Crypt hyperplasia is a common response to mucosal injury. It occurs, for example, following infection of the mucosa by cytolytic agents,[18-20] after radiation injury,[21] and in diseases such as tropical and celiac sprue.[22,23] Mechanisms initiating mucosal hyperplasia are, however, not well understood. Recent work indicates that the proliferation and differentiation of crypt–villus epithelium may be controlled by a feedback regulatory system.[21,24-26] Rijke and co-workers have hypothesized that such a feedback mechanism might stimulate proliferation of cells in the critical decision zone in response to reductions in the size of

the mature villus cell compartment.[25,26] It has been suggested that hormones, chalones, other humoral factors, and nutritional factors also help regulate the kinetics of epithelial turnover.[27-32] The role of putative feedback regulatory systems in the initiation of TIH and the potential influence of the etiologic agent on feedback regulation are speculative but pose interesting questions for future research.

References

1. Jonas AM, Tomita Y, Wyand S: Enzootic intestinal adenocarcinoma in hamsters. J Am Vet Med Assoc 147:1102–1108, 1965
2. Booth AD, Cheville NF: The pathology of proliferative ileitis of the golden hamster. Vet Pathol 4:31–44, 1967
3. Jacoby RO, Osbaldiston GW, Jonas AM: Experimental transmission of atypical ileal hyperplasia of hamsters. Lab Anim Sci 25:465–473, 1975
4. Jacoby RO: Transmissible ileal hyperplasia of hamsters. I. Histogenesis and immunocytochemistry. Am J Pathol 91:433–450, 1978
5. McDowell EM, Trump BF: Histologic fixatives suitable for diagnostic light and electron microscopy. Arch Pathol Lab Med 100:405–414, 1976
6. Mollenhauer HH: Plastic embedding mixture for use in electron microscopy. Stain Technol 39:111–114, 1964
7. Richardson KC, Jarett L, Finke EH: Embedding in epoxy resins for ultra-thin sectioning in electron microscopy. Stain Technol 35:313–323, 1960
8. Venable JH, Coggeshall RA: A simplified lead citrate stain for use in electron microscopy. J Cell Biol 25:407–408, 1965
9. Wagner JE, Owens DR, Troutt HF: Proliferative ileitis of hamsters: Electron microscopy of bacteria in cells. Am J Vet Res 35:249–252, 1973
10. Costerton JW, Ingram JM, Cheng K-J: Structure and function of the cell envelope of gram-negative bacteria. Bacteriol Rev 38:87–110, 1974
11. Rowland AC, Lawson GHK: Intestinal adenomatosis in the pig: Immunofluorescent and electron microscopic studies. Res Vet Sci 17:323–330, 1974
12. Rowland AC, Lawson GHK: Intestinal adenomatosis in the pig: Possible relationship with hemorrhagic enteropathy. Res Vet Sci 18:263–268, 1975
13. Lawson GHK, Rowland AC, Wooding P: The characterization of *Campylobacter sputorum* subspecies *mucosalis* isolated from pigs. Res Vet Sci 18:121–126, 1975
14. Takeuchi A: Electron microscope studies of experimental *Salmonella* infection. I. Penetration into the intestinal epithelium by *Salmonella typhimurium*. Am J Pathol 50:109–136, 1967
15. Takeuchi A, Formal SB, Sprinz H: Experimental acute colitis in the rhesus monkey following peroral infection with *Shigella flexneri*: An electron microscope study. Am J Pathol 42:503–529, 1968
16. Staley TE, Jones EW, Corley LD: Attachment and penetration of *Escherichia coli* into intestinal epithelium of the ileum of newborn pigs. Am J Pathol 56:371–397, 1969
17. Takeuchi A: Penetration of the intestinal epithelium by various microorganisms. Curr Top Pathol 54:1–27, 1971
18. Abrams GD, Schneider H, Formal SB, Sprinz H: Cellular renewal and mucosal morphology in experimental enteritis: Infection with *Salmonella typhimurium* in the mouse. Lab Invest 12:1241–1248, 1963
19. Takeuchi A, Sprinz H, LaBrec EH, Formal SB: Experimental bacillary dysentery. An electron microscopic study of the response of the intestinal mucosa to bacterial invasion. Am J Pathol 47:1011–1044, 1965

20. Biggers DC, Kraft LM, Sprinz H: Lethal intestinal virus infection of mice (LIVIM): An important new model for study of the response of the intestinal mucosa to injury. Am J Pathol 45:413–422, 1964
21. Withers HR: Regeneration of intestinal mucosa after irradiation. Cancer 28:75–81, 1971
22. Perera DR, Weinstein WM, Rubin CE: Symposium on pathology of the gastrointestinal tract. II. Small intestinal biopsy. Hum Pathol 6:157–217, 1975
23. Paduka HA: Recent functional interpretations of intestinal morphology. Gastroenterology 21:873–879, 1962
24. Galjaard H, Van der Meer-Fieggen W, Giesen J: Feedback control by functional villus cells on cell proliferation and maturation in intestinal epithelium. Exp Cell Res 73:197–207, 1972
25. Rijke RPC, Van der Meer-Fieggen W, Galjaard H: Effect of villus length on cell proliferation and migration in small intestinal epithelium. Cell Tissue Kinet 7:577–586, 1974
26. Rijke RPC, Plaisier H, Hoogeveen AT, Lamerton LF, Galjaard H: The effect of continuous irradiation on cell proliferation and maturation in small intestinal epithelium. Cell Tissue Kinet 8:441–453, 1975
27. Loran MR, Carbone IV: The humoral effect of intestinal resection on cellular proliferation and maturation in parabiotic rats. Gastrointestinal Radiation Injury. Nuclear Medicine and Biology Monograph No. 1. Edited by MF Sullivan. Amsterdam, Excerpta Media Foundation, 1968
28. Tilson MD, Wright HK: Adaptation of functioning and by-passed segments of ileum during compensatory hypertrophy of the gut. Surgery 67:687–693, 1970
29. Gleeson MH, Cullen J, Dowling RH: Intestinal structure and function after small bowel by-pass in the rat. Clin Sci Mol Med 43:731–742, 1972
30. Feldman EJ, Peters TJ, McNaughton J, Dowling RH: Adaptation after small bowel resection: Comparison of oral versus intravenous nutrition. Gastroenterology 66:691, 1974 (Abstr)
31. Brugel G: Presence of intestinal chalones in stem cells of renewing cell populations. Stem Cells: Renewing Cell Population. Edited by AB Cairnie. New York, Academic Press, Inc., 1976
32. Tutton PJM: Control of epithelial cell proliferation in the small intestine crypt. Cell Tissue Kinet 6:211–216, 1973

[*Illustrations follow*]

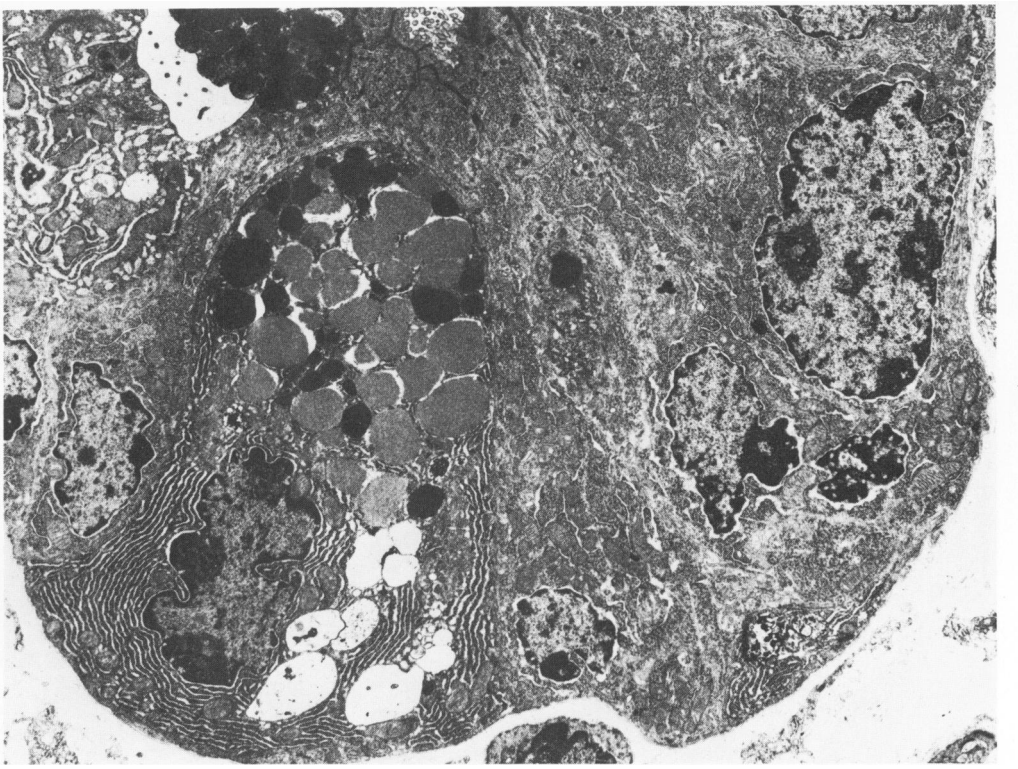

1

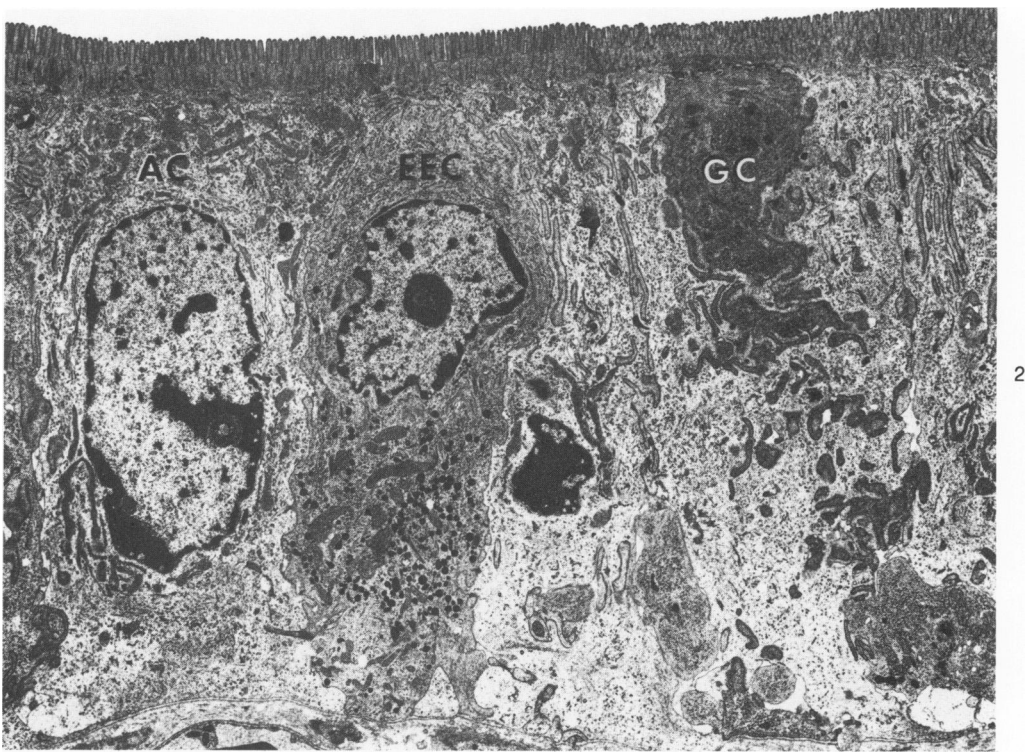

2

Figure 1—Crypt base from a control hamster. A Paneth cell containing large cytoplasmic inclusions and whorls of rough endoplasmic reticulum rests on the thin basement membrane at the crypt base. Undifferentiated cells (*right*) are pyramidal and contain many free ribosomes. (Uranyl acetate and lead citrate, × 4720) **Figure 2**—Villus epithelium from control hamster. At the left is a mature absorptive cell (*AC*) with Golgi bodies and short segments of rough endoplasmic reticulum. In the center, an enteroendocrine cell (*EEC*) contains characteristic small dense granules in the basal cytoplasm. At the right is the dense cytoplasm of a depleted goblet cell (*GC*). A brush border, composed of uniform tightly packed microvilli, covers the villus surface. (Uranyl acetate and lead citrate, × 4620)

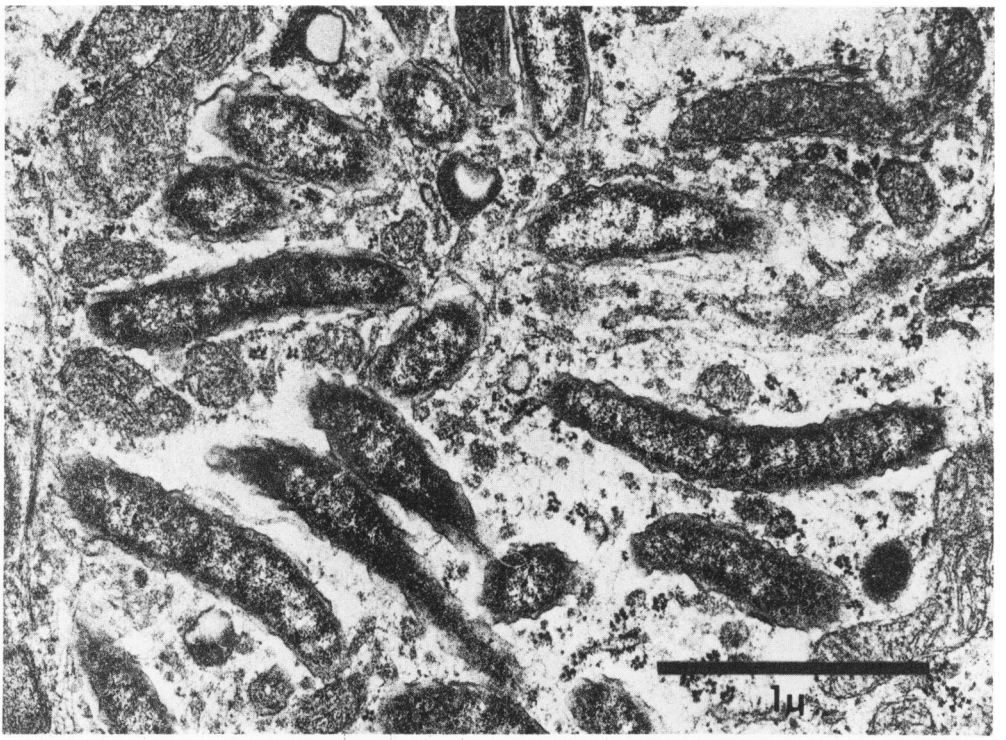

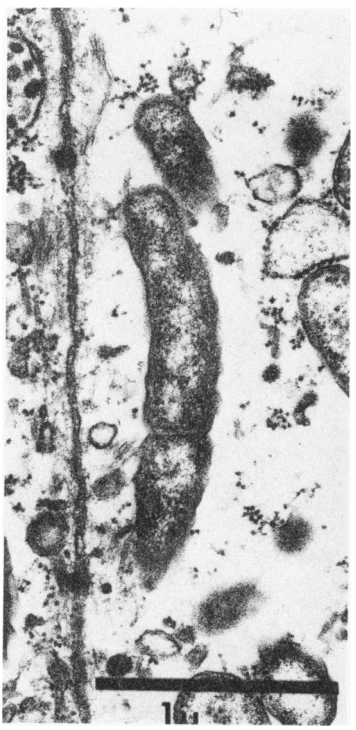

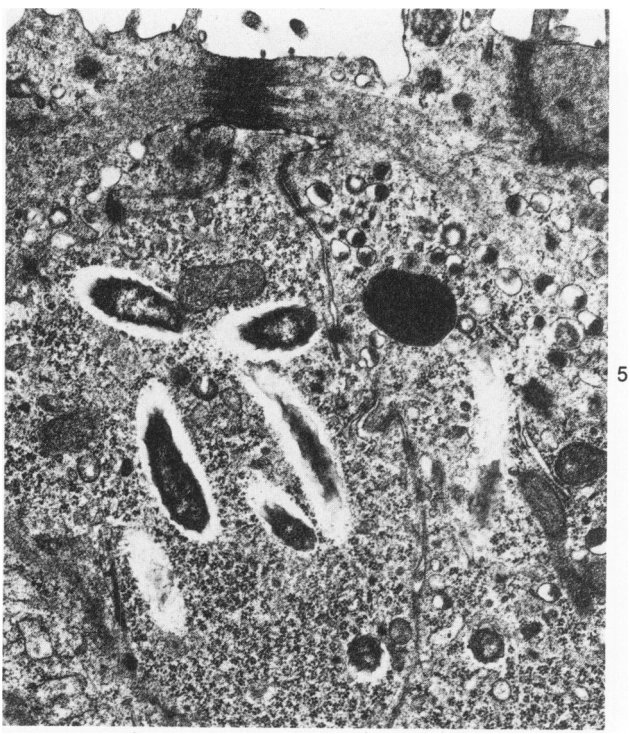

Figure 3—Bacteria in villus cell at 5 days. The bacteria are slightly curved rods surrounded by a double crenulated cell wall and are in intimate contact with host cytoplasm. Granules which resemble lysosomes lie near the bacteria, but fusion and secondary lysosomes are not seen. (Uranyl acetate and lead citrate, × 35,800) **Figure 4**—Intracytoplasmic bacteria undergoing binary fission. (Uranyl acetate and lead citrate, × 32,300) **Figure 5**—Bacteria in mid crypt cells at 5 days. A midbody at the lumen connects two recently divided cells. Daughter cells contain bacteria. The small vesicles with eccentric granules lying near the plasma membrane are commonly observed in undifferentiated crypt cells, and aggregated free ribosomes are numerous. (Uranyl acetate and lead citrate, × 18,840)

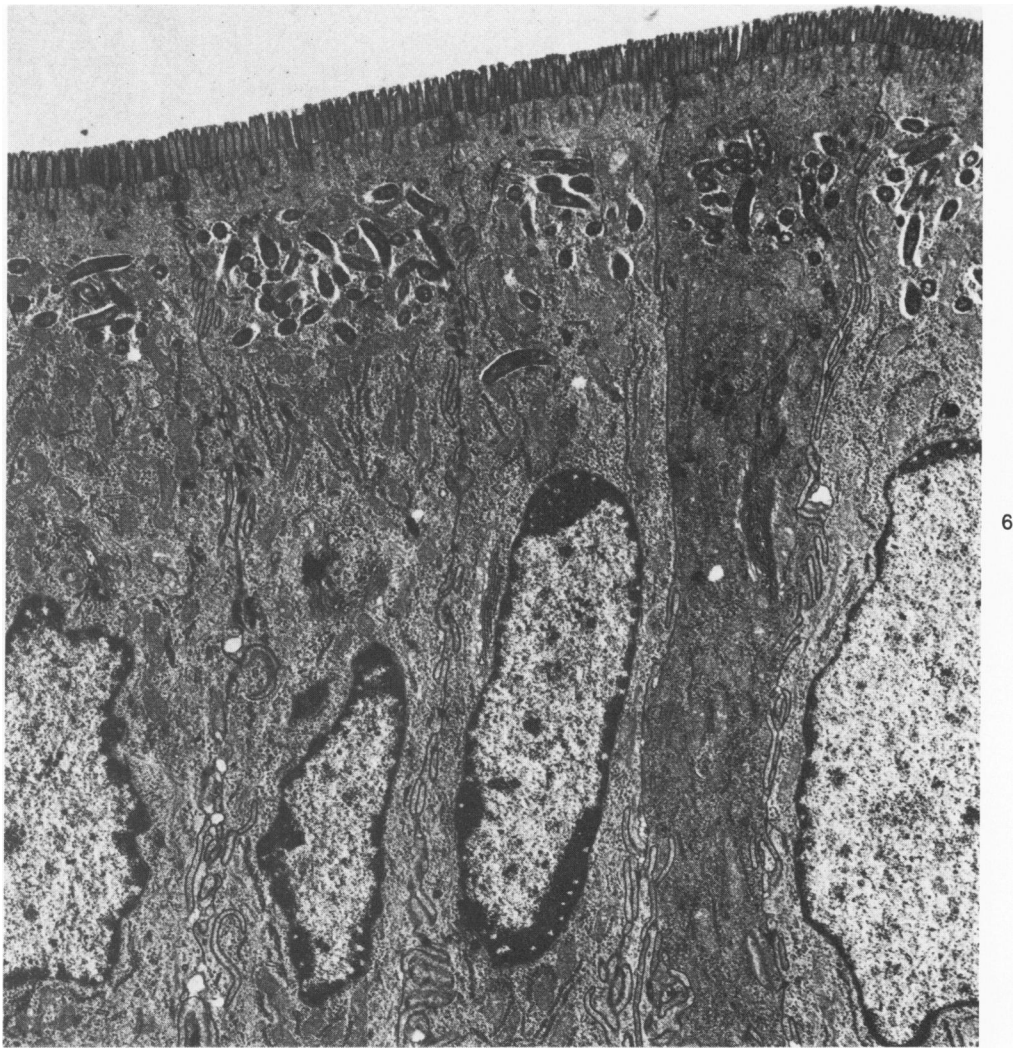

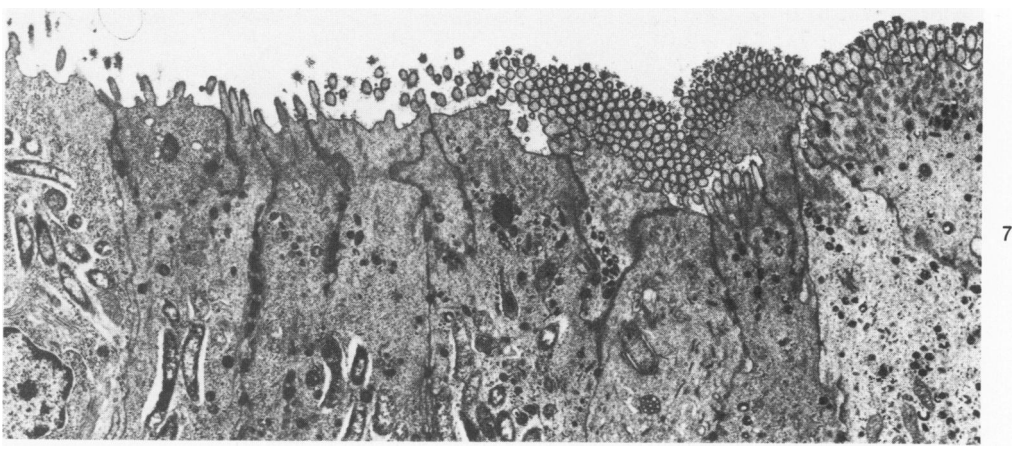

Figure 6—Columnar absorptive cells on villus surface of infected crypt-villus unit at 10 days. Variable numbers of bacteria, 9 to 34 per cell, occupy the apical cytoplasm of well-differentiated structurally normal villus epithelium. (Uranyl acetate and lead citrate, × 6400) **Figure 7**—Midcrypt area showing unusually sharp junction between infected and uninfected cells at 10 days. Infected cells at *left* have rudimentary microvilli typical of crypt base cells; uninfected cells at *right* have a more well-developed brush border, characteristic of mid to upper crypt regions. (Uranyl acetate and lead citrate, × 7560)

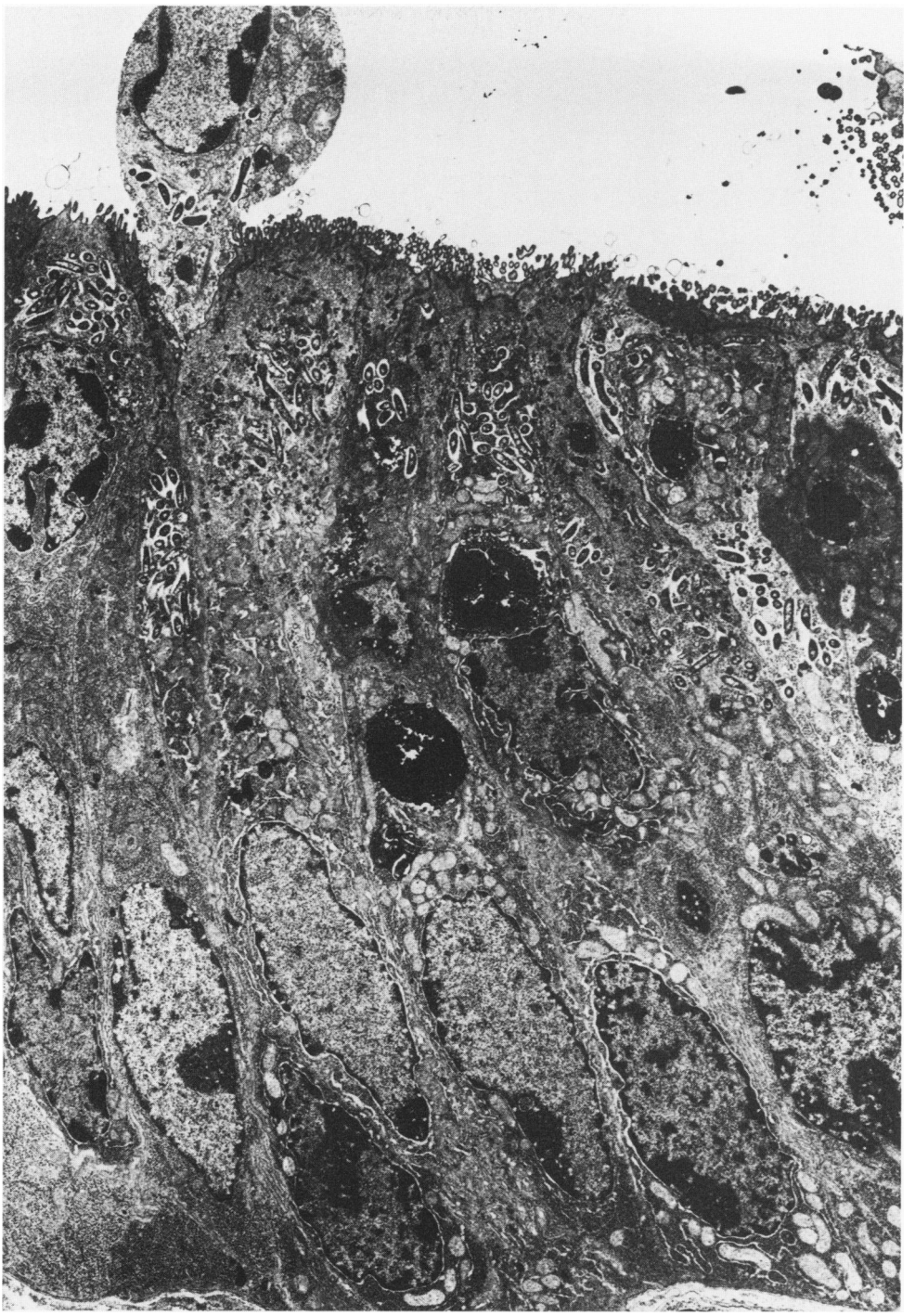

Figure 8—Hyperplastic epithelium in upper crypt region at 10 days. Cells are elongated and pseudostratified and contain bacteria in apical cytoplasm. Large dense secondary lysosomes contain remnants of phagocytized cells and bacteria. A necrotic cell, containing bacteria, is being extruded into the lumen. (Uranyl acetate and lead citrate, × 4350)

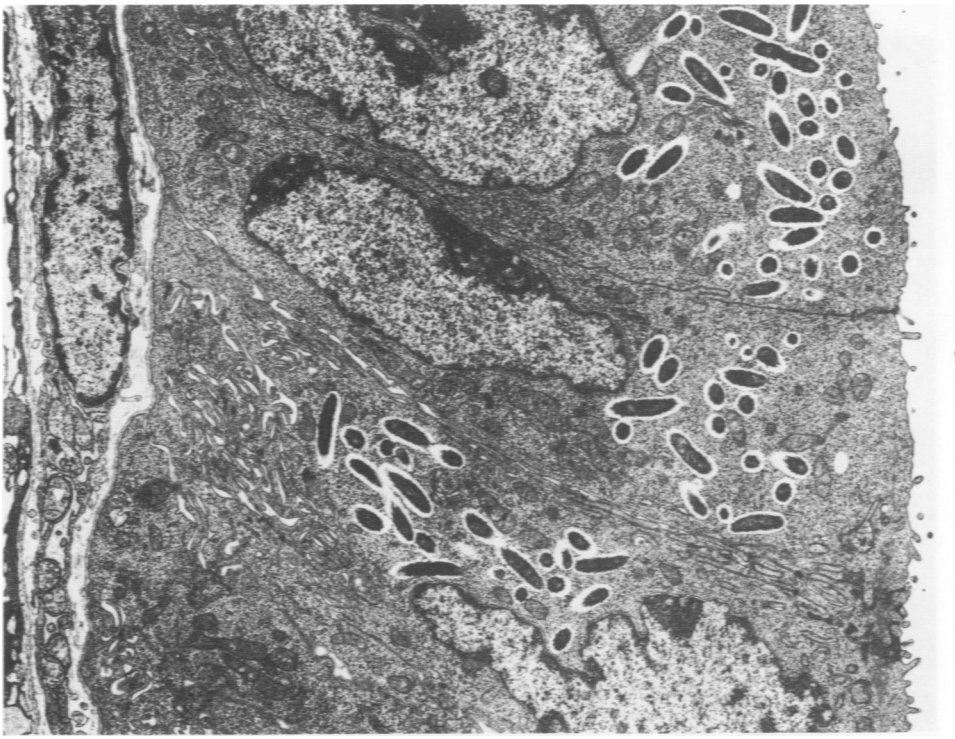

9

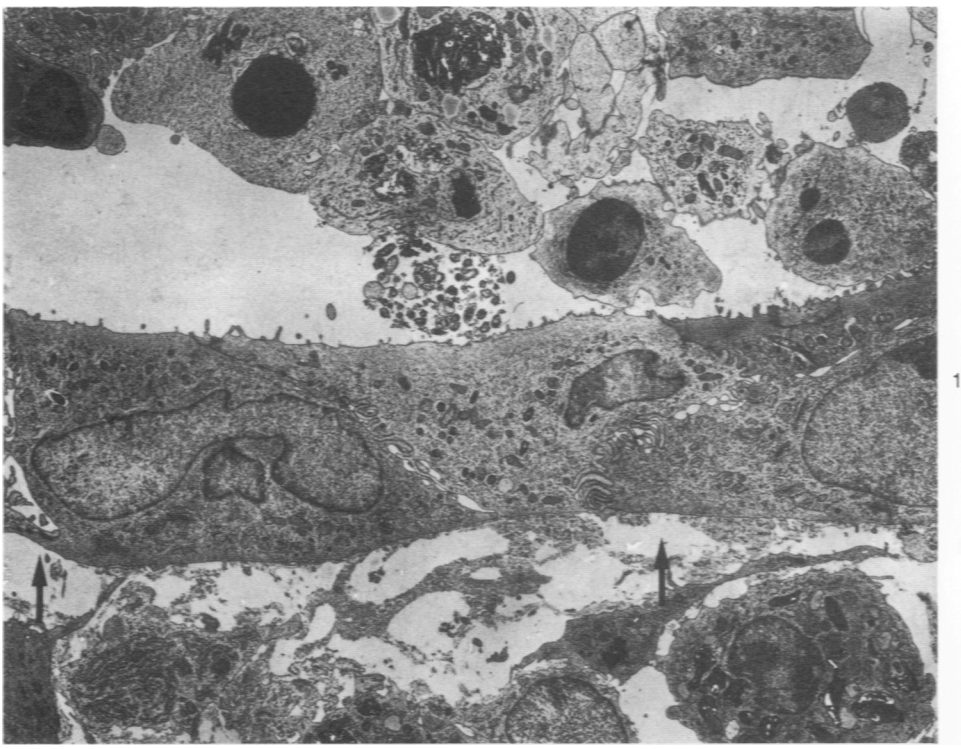

10

Figure 9—Hyperplastic villus epithelium at 14 days. Columnar cells with interdigitating lateral membranes abut a continuous basement membrane. Numerous bacteria occupy the apical cytoplasm which is otherwise composed almost entirely of free ribosomes and scattered mitochondria. Only a few rudimentary microvilli are seen at the luminal surface. (Uranyl acetate and lead citrate, × 6480) **Figure 10**—Portion of crypt epithelium penetrating the inner muscle layer. Flattened undifferentiated cells, containing a few bacteria abut a discontinuous basement membrane (*arrows*). Macrophages containing bacterial debris lie within the lumen and have infiltrated the muscle tissue around the crypt. (Uranyl acetate and lead citrate, × 3690)

11

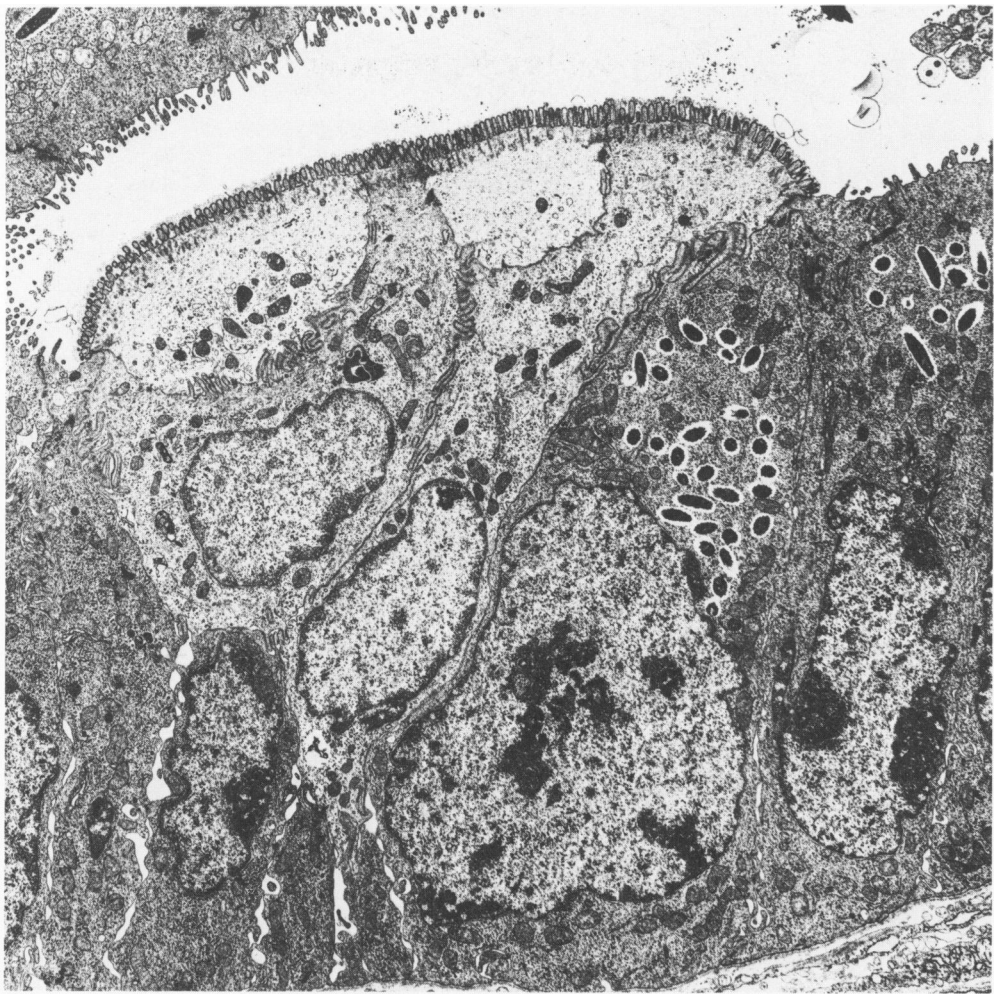

12

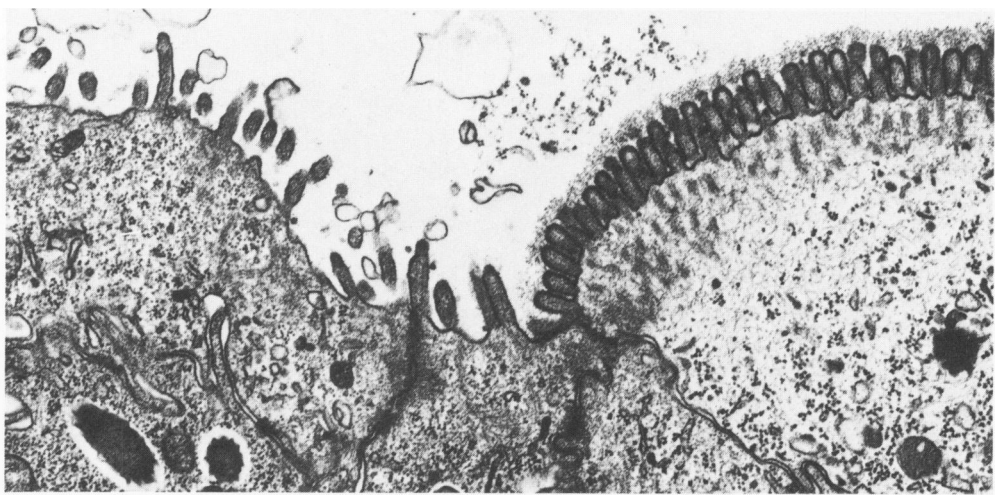

Figure 11—Differentiating cells on lower villus surface at 25 days. This oblique section through a crypt shows four cells, free of bacteria, undergoing differentiation. Neighboring infected cells are immature. (Uranyl acetate and lead citrate, × 5100) **Figure 12**—Differentiation of the brush border, glycocalyx, and terminal web in uninfected cells adjacent to immature infected cells in an area similar to that shown in Figure 11. (× 17,640)

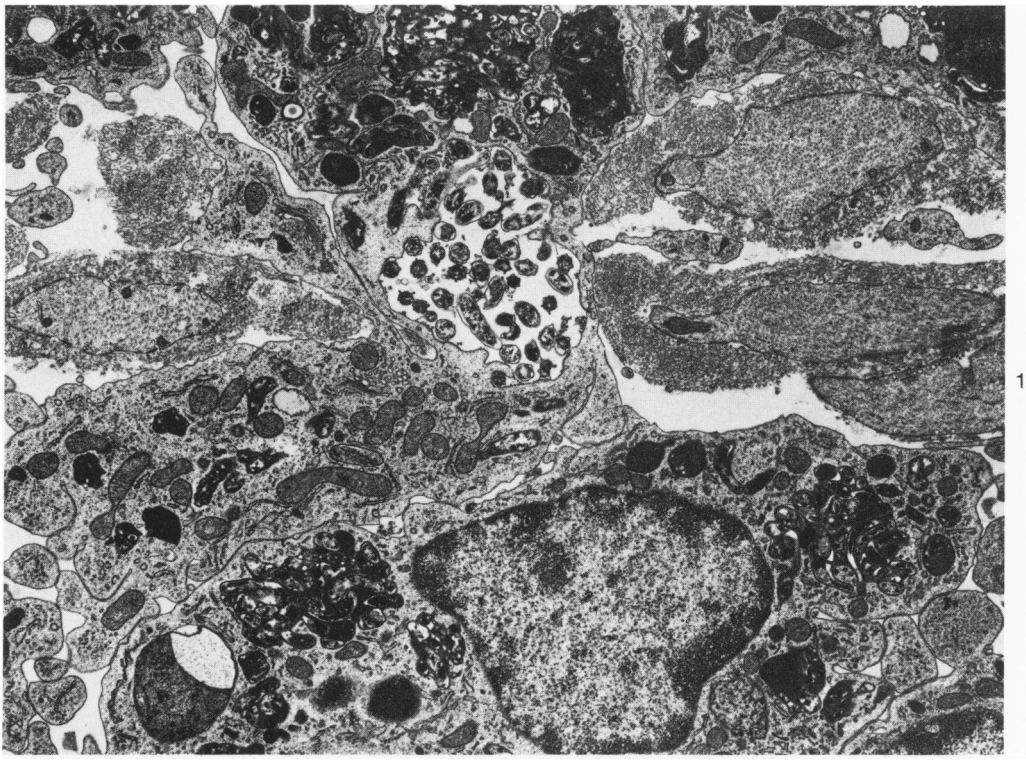

13

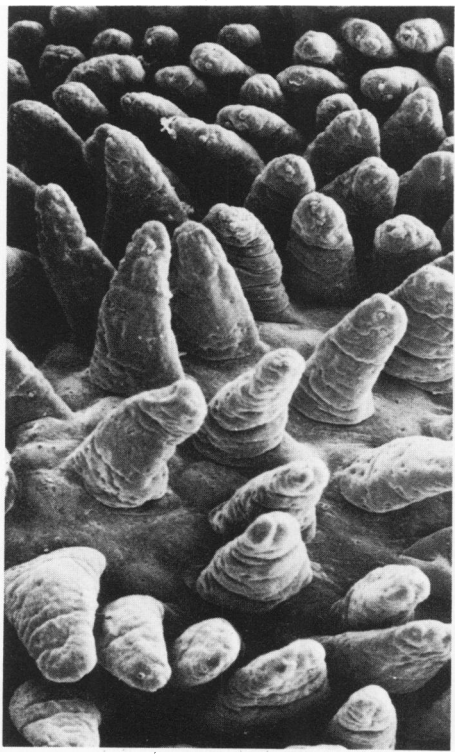

14

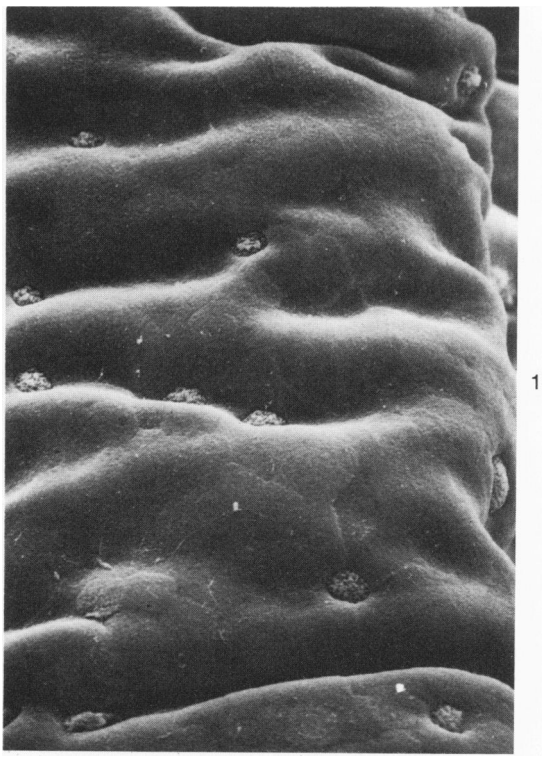

15

Figure 13—Macrophages infiltrating muscle layers. They contain bacteria in a phagocytic vacuole and in secondary lysosomes. (Uranyl acetate and lead citrate, × 8050) **Figure 14**—Scanning micrograph of ileal mucosa from a control hamster. Villi are slightly flattened and taper toward the tips. Narrow crypt openings punctuate intervillus spaces, and transverse infoldings occur along villus surfaces. (× 117) **Figure 15**—Higher magnification of normal villus surface. Goblet cells are prominent, and the polygonal outline of absorptive cells can be discerned. A tightly packed layer of microvilli covers the villus surface. (× 1280)

16

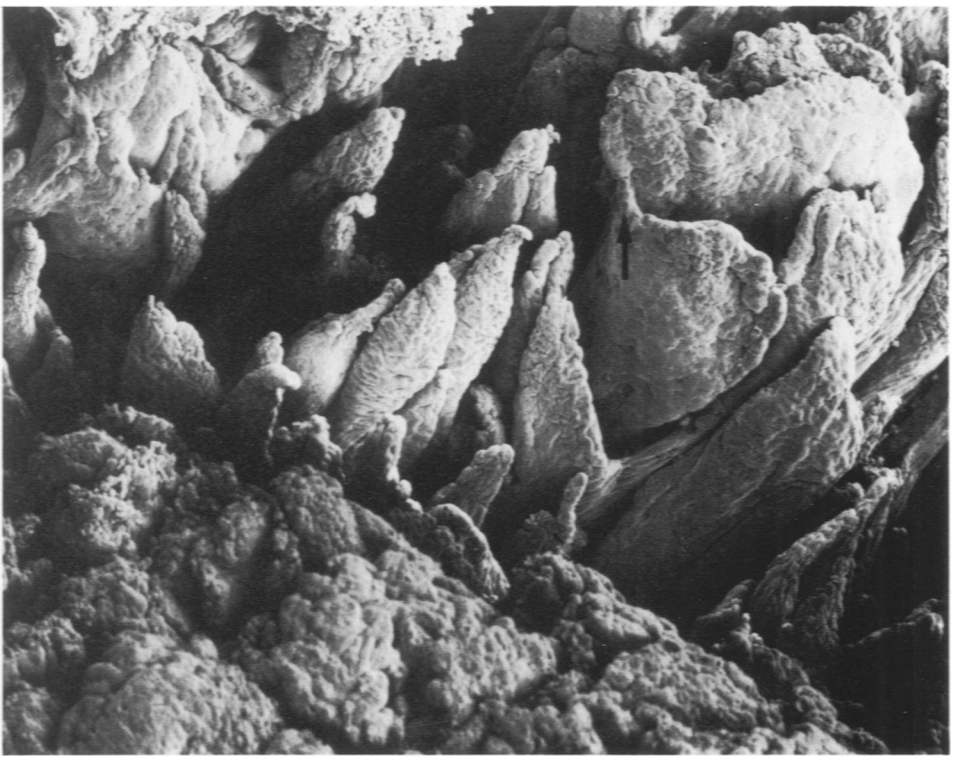

17

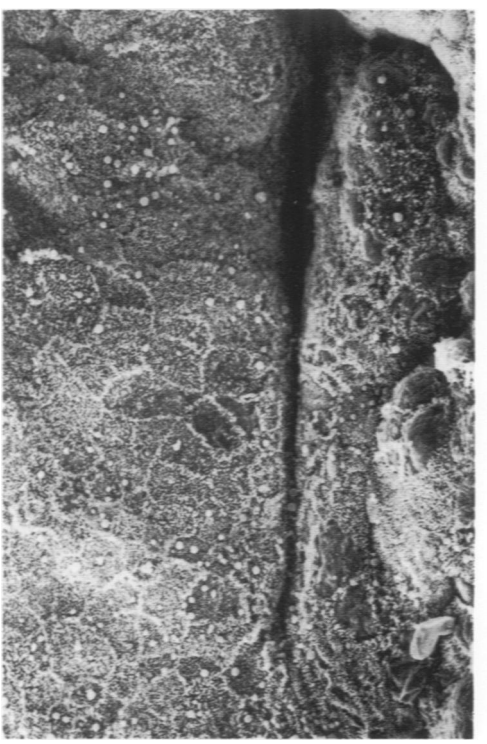

18

Figure 16—Lesion at 26 days. There is a sharp demarcation between plateaus that have formed by fusion of villus apices (*lower left*) and areas composed of large, overlapping, leaf-like villus structures interconnected by cellular bridges (*arrow*). (× 123) **Figure 17**—Severe hyperplasia at 23 days. Villus structure is distorted, and the villus–crypt junction (*arrows*) is elevated above the basal lamina. (× 110) **Figure 18**—Higher magnification of surface of hyperplastic villus. Cell borders are clearly visible through the layer of irregularly distributed microvilli. Cells are generally smaller than in the controls. (× 1290)